

May 4, 2000

APPLICATION OF THE LIMIT-CYCLE MODEL TO STAR FORMATION HISTORIES IN SPIRAL GALAXIES: VARIATION AMONG MORPHOLOGICAL TYPES

HIROYUKI HIRASHITA¹ AND HIDEYUKI KAMAYA

Department of Astronomy, Faculty of Science, Kyoto University, Sakyo-ku, Kyoto 606-8502, Japan

hirasita@kusastro.kyoto-u.ac.jp

ABSTRACT

We propose a limit-cycle scenario of star formation history for any morphological type of spiral galaxies. It is known observationally that the early-type spiral sample has a wider range of the present star formation rate (SFR) than the late-type sample. This tendency is understood in the framework of the limit-cycle model of the interstellar medium (ISM), in which the SFR cyclically changes in accordance with the temporal variation of the mass fraction of the three ISM components. When the limit-cycle model of the ISM is applied, the amplitude of variation of the SFR is expected to change with the supernova (SN) rate. Observational evidence indicates that the early-type spiral galaxies show smaller rates of present SN than late-type ones. Combining this evidence with the limit-cycle model of the ISM, we predict that the early-type spiral galaxies show larger amplitudes in their SFR variation than the late-types. Indeed, this prediction is consistent with the observed wider range of the SFR in the early-type sample than in the late-type sample. Thus, in the framework of the limit-cycle model of the ISM, we are able to interpret the difference in the amplitude of SFR variation among the morphological classes of spiral galaxies.

Subject headings: galaxies: evolution — galaxies: ISM — galaxies: spiral — ISM: evolution — stars: formation

1. INTRODUCTION

In this paper, we propose a scenario of star formation histories in giant spiral galaxies. Our standpoint is based on a very interesting observational result presented in Kennicutt, Tamblyn,

¹Research Fellow of the Japan Society for the Promotion of Science.

& Congdon (1994, hereafter KTC). According to their sample galaxies, there is a difference in present star-formation activity among morphological types of spiral galaxies. This is found in KTC (the third paragraph of their §5.2). The early-type spiral galaxies have a one-order-of-magnitude range in b , which denotes the present-to-past ratio of star-formation rate (SFR), as being $b = 0.01$ – 0.1 . On the other hand, $b = 0.5$ – 2 , a range of just a small factor, in the late-type spiral sample. Moreover, in the framework of the scenario proposed in this paper, we can incorporate another relevant observational result; the difference of supernova (SN) rate among the galactic morphology (Cappellaro et al. 1993).

Not only KTC, but also Tomita, Tomita, & Saitō (1996) found a difference in present star-formation activity among different morphological types of spiral galaxies (see also Devereux & Hameed 1997). Tomita et al. (1996) commented that this variation may be a short-term change in the SFR in spiral galaxies and the duration of an episode of star formation activity is less than 10^8 yr.

Kamaya & Takeuchi (1997, hereafter KT97) independently put an observational interpretation about the difference in present star-formation activity among morphological types. They pointed out that the short duration of star formation proposed by Tomita et al. (1996) may indicate that the interstellar medium (ISM) in a spiral galaxy is a non-linear open-system. That is, they suggested that the duration may result from the period of a limit cycle of mass exchange among various phases of the ISM (see Ikeuchi & Tomita 1983, hereafter IT83, for the limit-cycle behavior). If the ISM in a galaxy is regarded globally to be a non-linear open-system, the evolution of whole ISM on a galaxy-wide scale may result in the limit-cycle star formation history. Indeed, the variance of the star formation activities of spiral galaxies can be understood as a short-term ($\lesssim 10^8$ yr) variation of their activities. Recent result by Rocha-Pinto et al. (2000) suggests that the Galactic star formation history indeed shows such a galaxy-wide variability.

KT97’s discussion was based on the sample of Tomita et al. (1996). In the subsequent discussions, we re-examine KT97’s proposal more quantitatively than their original considerations through a proper comparison with KTC. Moreover, we check whether their scenario is consistent with the difference of SN rate among the morphological types of spirals, since the amplitude of the limit-cycle orbit is determined by the SN rate (§4). Thus, we can state clearly our motivation here. We aim to interpret the difference in star formation history among morphological types in the framework of the limit-cycle model of ISM in spiral galaxies.

According to a review by Ikeuchi (1988), he and his collaborators indicated that we might understand the dynamical evolution of the ISM on a galaxy-wide scale if we could describe galaxies as nonlinear open systems (see also Nozakura & Ikeuchi 1984, 1988). Here, we stress that one type of their models, the limit-cycle model, indicates a periodic star formation history (KT97). A more elaborate model is also proposed by Tainaka, Fukazawa, & Mineshige (1993). To understand the behavior of star formation activity of spiral galaxies, we focus on this interesting hypothetical behavior of the ISM. Adopting the limit-cycle model, KT97 insisted that the amplitude of the

cyclic part of the SFR, Ψ' , should be larger than the SFR of the quiescent era, $\bar{\Psi}$. Moreover, adopting a Schmidt (1959) law of index of 2, they predicted that the amplitude ratio of Ψ' s, defined as $\text{Max}(\Psi')/\text{Min}(\Psi')$, should be ~ 50 . Here, $\text{Max}(\Psi')$ and $\text{Min}(\Psi')$ indicate the maximum and minimum values of Ψ' , respectively. However, since $\text{Max}(\Psi')/\text{Min}(\Psi')$ depends on the characteristic parameters for the limit-cycle model (IT83; or §2 in this paper), we re-examine the amplitude for various parameters in this paper.

Throughout this paper, thus, we discuss the difference in the amplitude of cyclic star formation among the three morphological types of spiral galaxies (Sa, Sb, and Sc) along with the limit-cycle model. In the next section, we review the limit-cycle model of the ISM. In §3, we estimate the amplitude of cyclic SFR, and interpret the difference in the amplitude via the limit-cycle model. In §4, a consistent scenario for the time variation of SFR is proposed. In the final section, we summarize our considerations and present some discussions.

2. CYCLIC STAR FORMATION HISTORY

Since our discussions are based on mainly KTC in this paper, we summarize firstly KTC. KT97 is also reviewed. Although KT97 discussed Tomita et al. (1996), their argument on the duration and the behavior of star formation activity is not altered even if we are based on KTC.

2.1. KTC's Sample and KT97's Interpretation

Treating a data set of $\text{H}\alpha$ equivalent widths of galactic disks with various morphologies, KTC has shown that the star formation activities present a wide spread for each morphological type (KTC's Fig. 6). They derived b parameter which indicates the ratio of the present SFR to the past-averaged SFR.

Based on KT97, we re-interpret Figure 6 in KTC: The KTC's wide dispersion of the star formation activity is interpreted as evidence for a periodic star-formation history on the scale of a giant galaxy. If galaxies have the same morphological type and the same age, such a large scatter as that in Figure 6 of KTC should not appear for near constant or monotonically declining SFRs. However, if cyclic star formation occurs in any spiral galaxy, we can easily understand why such a large scatter emerges. If the period of the cyclic star formation is several times 10^7 years, the dispersions in KTC's Figure 6 do not contradict the hypothesis of KT97 by setting $b = \Psi'/\bar{\Psi}$, where Ψ' and $\bar{\Psi}$ are the cyclic and past-averaged SFR, respectively.

Indeed, such a periodic star formation history is proposed by Ikeuchi (1988) as cited by KT97. His discussion is based on the limit-cycle behavior of the fractional mass of each ISM shown by IT83. If the fractional component of the cold gas, where stars are formed, cyclically changes on a short timescale ($\sim 10^7$ – 10^8 yr), the SFR also varies cyclically. Thus, we review the formulation by

IT83 in the next subsection.

2.2. Limit-Cycle Model of ISM

We review the limit-cycle model for the ISM proposed by IT83 (see also Scalo & Struck-Marcell 1986). The model has been utilized to interpret Tomita et al. (1996) (KT97). The limit-cycle behavior emerges if we treat the ISM as a non-linear open system. As long as the ISM is a non-linear open system, it spontaneously presents a dissipative structure (Nozakura & Ikeuchi 1984).

First of all, we should note that the galaxy disk is treated as one zone. The interstellar medium is assumed to consist of three components each with its temperature T and density n (McKee & Ostriker 1977); the hot rarefied gas ($T \sim 10^6$ K, $n \sim 10^{-3}$ cm $^{-3}$), the warm gas ($T \sim 10^4$ K, $n \sim 10^{-1}$ cm $^{-3}$), and the cold clouds ($T \sim 10^2$ K, $n \sim 10$ cm $^{-3}$). The fractional masses of the three components are denoted by X_h , X_w , and X_c , respectively. A trivial relation is

$$X_h + X_w + X_c = 1. \quad (1)$$

The following three processes are considered in IT83 (see also Habe, Ikeuchi, & Tanaka 1981): [1] the sweeping of the warm gas into the cold component at the rate of $a_* X_w$ ($a_* \sim 5 \times 10^{-8}$ yr $^{-1}$); [2] the evaporation of cold clouds embedded in the hot gas at the rate of $b_* X_c X_h^2$ ($b_* \sim 10^{-7}$ – 10^{-8} yr $^{-1}$); [3] the radiative cooling of the hot gas by mixing with the ambient warm gas at the rate of $c_* X_w X_h$ ($c_* \sim 10^{-6}$ – 10^{-7} yr $^{-1}$). Writing down the rate equations and using equation (1), IT83 obtained

$$\frac{dX_c}{d\tau} = -BX_c X_h^2 + A(1 - X_c - X_h), \quad (2)$$

$$\frac{dX_h}{d\tau} = -X_h(1 - X_c - X_h) + BX_c X_h^2, \quad (3)$$

where $\tau \equiv c_* t$, $A \equiv a_*/c_*$, and $B \equiv b_*/c_*$.

The solutions of equations (2) and (3) are classified into the following three types (IT83):

- [1] $A > 1$; all the orbits in the (X_c, X_h) -plane reduce to the node $(0, 1)$ (node type),
- [2] $A < 1$ and $B > B_{\text{cr}}$; all the orbits reduce to a stable focus $[(1 - A)/(AB + 1), A]$ (focus type),
- [3] $A < 1$ and $B < B_{\text{cr}}$; all the orbits converge on a limit-cycle orbit (limit-cycle type),

where $B_{\text{cr}} \equiv (1 - 2A)/A^2$. Obviously, case [3] is important if we wish to predict a cyclic star formation history. According to the summary of the limit-cycle model by Ikeuchi (1988), the period of a cycle is several times 10^7 years, as depicted in his Figure 4. Since this period is much smaller than the characteristic timescales in galaxy evolution such as the gas consumption timescale

(> 1 Gyr: KTC’s τ_R), the cyclic change of SFR will produce a scatter in the observed star formation activities in spiral galaxies even if their ages are similar.

3. OSCILLATORY MODEL OF SFR

3.1. Model Description

According to KT97, we use a simple description to test our discussion. First, we define the present quiescent component of the SFR as $\bar{\Psi}$ and the oscillatory component of the SFR as Ψ' . Then, the total SFR is denoted as

$$\Psi = \bar{\Psi} + \Psi'. \quad (4)$$

Our definitions are adequate when the period of oscillation of the SFR is much smaller than the cosmic age (e.g., Sandage 1986). According to Schmidt (1959), the SFR in a galaxy is approximately expressed as $\text{SFR} \propto n^p$ ($1 < p < 2$), where n is the mean gas density of the galaxy. If we interpret n as the gas density of a cold cloud, which can contribute to the star formation activity, we expect the oscillatory part of the SFR to be

$$\Psi' \propto X_c^{1.5}, \quad (5)$$

where we have assumed that $p = 1.5$ (Kennicutt 1998). Using this relation and equations (2) and (3), the variation of the star formation activity (i.e., Ψ' as a function of τ) is calculated. For example, according to Figure 6 in Ikeuchi (1988), this mass fraction of the cold gas, X_c , can vary from ~ 0.1 to ~ 0.9 . Thus, we expect the magnitude of the variation of Ψ' to be about two orders of magnitude during one period of the oscillation.

Since our model follows IT83, the structure of a model galaxy is hypothesized to be one-zone, that is, the local phenomena of the ISM are averaged in space. The simplicity of the one-zone approximation gives the advantage that the background physical processes are easy to see. Moreover, even though the effect treated in this paper and IT83 may be local, a “global” (i.e., galactic-scale) dissipative structure of the ISM emerges (Nozakura & Ikeuchi 1984), as long as a galaxy is assumed to be a non-linear open system (Nicolis & Prigogine 1977). Thus, as a first step, we treat a model galaxy as being a one-zone object which is a non-linear open system.

Habe et al. (1981) stated in their §7 that for the one-zone assumption to be acceptable it is necessary that the mean distance between supernova remnants (SNRs) be less than 100 pc (if a characteristic lifetime of SNRs of $\tau_{\text{life}} \sim 10^7$ yr and a mean expansion velocity of 10 km s⁻¹ are adopted). This is because the SNRs should affect the whole disk for the one-zone treatment. The distance of less than 100 pc means that there are $N \sim 10^4$ SNRs in a galaxy disk, if the disk size of 10 kpc is assumed. This number is possible if SNe occur every 10^3 yr ($\tau_{\text{life}}/N \sim 10^7$ [yr]/ 10^4). Considering that the SN rate in a spiral galaxy is typically 1/100–1/50 yr⁻¹ (Cappellaro

et al. 1993), the mean distance between SNRs is less than 100 pc even if 10–20 massive stars are clustered in a region.

Indeed, from the observational viewpoint, Rocha-Pinto et al. (2000) have shown that the star formation history of the Galaxy does present a short-term variability whose timescale is less than ~ 1 Gyr (see also Takeuchi & Hirashita 2000). Though they adopted the sample stars in the solar neighborhood, they showed by estimating the diffusion time of the stars that the sample represents the stars in the Galaxy-wide scale. Based on this observational evidence as well as the discussions in the previous two paragraphs, we accept the one-zone treatment by IT83 and apply it to the ISM on a galactic-wide scale.

Once we accept the one-zone treatment, we need global observational measures of a galactic disk to examine our scenario. In this paper, the $H\alpha$ equivalent width in KTC is the global physical parameter. KTC declared that their data excluded the bulge component and that the disk component is uncontaminated.

3.2. Application to KTC

For the comparison between the model prediction and the observational data, we relate b defined in KTC (the ratio of the present SFR to the past-averaged SFR) to the model prediction. The parameter b is calculated from the equivalent width of $H\alpha$ emission. According to KT97, we can assume that $b \simeq \Psi'/\bar{\Psi}$ if the large variance of b in Figure 6 of KTC originates from a short-term variation. We combine the IT83’s model with the star formation history via the Schmidt law (equation 5). For example, when $X_c = 0.1$ at the minimum SFR and $X_c = 0.7$ at the maximum (Fig. 1 of IT83), the value of X_c^p changes from 0.03 to 0.59 during the cycle if $p = 1.5$. Accordingly, we find that the maximum SFR is about 20 times larger than the minimum SFR, since Ψ' is proportional to X_c^p (equation 5). Thus, using the cyclic star-formation scenario, we find the maximum of b also becomes 20 times larger than the minimum b in this numerical example.

To summarize, the large variance of b in Figure 6 of KTC is naturally derived through the Schmidt law, if the limit cycle model is a real evolutionary picture of ISM. In the next section, we examine this point more precisely, in order to reproduce the variance of star formation activities for each morphological type of spiral galaxies. In the following discussions, we examine $\text{Max}(\Psi')/\text{Min}(\Psi')$, where $\text{Max}(\Psi')$ and $\text{Min}(\Psi')$ are maximum and minimum values of the oscillatory SFR (the maximum and minimum are defined by the maximum and minimum star formation rates during a period of the limit cycle, respectively), and thus $\text{Max}(\Psi')/\text{Min}(\Psi') \equiv \text{Max}(X_c^p)/\text{Min}(X_c^p)$. In the rough estimate in the previous paragraph, $\text{Max}(\Psi')/\text{Min}(\Psi')$ is 20 with $p = 1.5$. Here, we define

$$F_c \equiv \frac{\text{Max}(\Psi')}{\text{Min}(\Psi')}, \quad (6)$$

for convenience in the subsequent sections. Using this relation and equations (2) and (3), the

Table 1. F_c as a function of A and B .

		B			
		0.5	1.0	1.5	2.0
A	0.32	355	137	61	29
	0.34	129	52	24	10
	0.36	57	23	9	3
	0.38	27	10	4	—
	0.40	15	4	—	—

Note. — We show the value of F_c if $B < B_c$ (the condition for the limit-cycle behavior) is satisfied. Otherwise, ‘—’ is marked. See text for the definitions of quantities.

variation of the star formation activity (i.e., Ψ' as a function of τ) is calculated, and F_c is evaluated finally.

4. SCENARIO OF LIMIT-CYCLE STAR FORMATION

To propose a scenario of star formation history for spiral galaxies based on the limit-cycle model, let us start with a very interesting observational result. According to KTC, the early-type sample has a larger variance of SFR than the late-type sample. As a first step, we reconstruct this observational tendency in the framework of IT83. Then, we perform several numerical analyses to examine parameters which implement the limit-cycle oscillation of the cold phase of the ISM. For the ISM in spiral galaxies, the full possible ranges of the parameters of A and B (e.g., Habe et al. 1981) are $A = a_*/c_*$ of ~ 0.05 to ~ 0.5 and that $B = b_*/c_*$ of ~ 0.01 to ~ 1 , respectively. In the following discussions, we focus on the parameter sets for the limit-cycle type (case [3] in §2.2).

Two of the results of differently parametrized limit-cycle behavior are displayed in Figures 1a–1b, where the SFRs are normalized to the minimum SFR. In Figure 1a, we find an amplitude (F_c) of about 10, which might correspond to the result of the Sa sample in KTC. Figure 1b corresponds to the amplitude of about 4 for Sc in KTC.

Clearly, the difference in the amplitude between the Sa and Sc galaxies for the KTC data sets can be reproduced via the models which yield Figures 1a and 1b. We also present F_c for various A and B in Table 1, from which we observe that the value of F_c is more sensitive to A than to B . Indeed, from the rough estimate, $\delta F_c/\delta A \sim -133/0.08 \sim -1600$ for $B = 1.0$ and $\delta F_c/\delta B \sim -119/1.5 \sim -80$ for $A = 0.34$. Thus, the two figures are presented for different values of A . Here, we state an important point: The early-type spiral galaxies favor a small A , while the late-type ones are consistent with a large A .

The variation of the amplitude in accordance with A and B is qualitatively interpreted as

follows. Small A (or small B) indicates that the transition from the warm to the hot component (or the cold to the warm component) is inefficient. Thus, when A (or B) is small, we must wait for X_w (or X_c) to become large before the phase transition can become important, since the transition rate is described by AX_w (or $BX_cX_h^2$). Thus, the amplitude and the period become large for small A (or B). This interpretation of the relation between A (or B) and the amplitude is qualitatively robust. This means that the scenario proposed in this paper is unchanged even if a more elaborate model such as Ikeuchi, Habe, & Tanaka (1984) is used.

As a next step, we examine the SFR variance via the effect of A . According to the definition of A in §2.2, we expect a larger rate of SNe for large A (e.g., Sc) than for small A (e.g., Sa). Then, the result in the previous paragraph predicts an important point that the early-type spiral galaxies have smaller *present* SN rate than the late-type spirals. This is confirmed in the following two points:

[1] The higher SFR per unit optical luminosity in later type spiral galaxies (Figure 6 of KTC) indicates that the Type II SN rate per unit optical luminosity is higher in later types. Thus, it is natural in the context of our model that the late-type spirals have larger A than the early-types.

[2] The expected trend of the SN rate for early-to-late types has been found by Cappellaro et al. (1993). They examine the SN rate per blue luminosity in various types of spirals, and present a summary of their results in their Table 4. We can confirm via their Table 4 that our scenario of limit-cycle SFR is consistent with the observational trend of SN rate as the galactic morphology varies. Moreover, the present SFR is reflected by the present rate of Type II SNe. According to Cappellaro et al., Sc-types show higher Type II SN rates than Sa types. Then, we can infer that the SFR of Sc galaxies is larger than that of Sa galaxies, which is compatible with Figure 6 of KTC.

From these pieces of evidence, we find a consistent picture of the SFR variance in the spiral sample as a function of morphology via the scenario of the limit-cycle star formation history. We note that the large gas-to-stars mass ratio in late-type spiral galaxies is probably the reason for the large SFR, and that a larger mean SFR yields a smaller variance because of a larger SN rate.

The trend of F_c with varying B is also consistent with the different SN rates among morphological types. Since B physically means the efficiency of the evaporation of the cold component via conduction (one of the so-called SN feedback effects), B increases with increasing SN rate. Because a large value of B tends to reduce F_c as can be seen in Table 1, a small F_c is caused when the SN rate is large. Thus, from a similar argument to that in the previous paragraph, late-type spiral galaxies ought to have small values of F_c . Considering the sensitivity of F_c to A (§4), however, we insist that A , not B , is the dominant contributor to the determination of the amplitude F_c .

To be fair, the picture presented in this paper may not be the unique interpretation of the variation of SFR. A stochastic fluctuation may easily reproduce the observed scatter of SFR in the KTC’s sample as commented in §5.2.

5. SUMMARY AND IMPLICATIONS

5.1. Summary

In this paper, we have demonstrated that the large variety of SFR in spiral sample in KTC may result from the limit-cycle evolution of ISM as suggested by KT97. We present this more quantitatively by using the numerical modeling by IT83 and explain the difference in the range of SFR between morphological types. It is known observationally that the early-type spiral sample has a wider range of the present SFR than the late-type sample (KTC). In our framework of the limit-cycle scenario of star-formation history in spiral galaxies, the early-types should show a more evident time variation of the SFR than the late-types to be consistent with the fact that Sc galaxies has the higher present SN rate than Sa galaxies (§4). Thus, the limit-cycle model by Ikeuchi and his collaborators provides a consistent picture of the ISM evolution for any type of spiral galaxies.

5.2. Implications

What is the underlying physical mechanism responsible for the variation in A and B ? Since A and B are related to the Type II SN rate, this question reaches the most basic and unsolved question: What is the physical mechanism responsible for the different star formation activities among morphological types? First of all, recall that the later spirals have larger bulge-to-disk ratio than the earlier spirals. This can mean that the net volume of disk of the later spirals is larger than that of the earlier spirals. Once we accept the larger volume of disk of the later spiral galaxies, we expect that Type II SN rate per galaxy is higher in the late types than in the early types because of the large disk, where on-going star formation is generally observed. Moreover, the parameter c_* is determined from the mixing rate between the warm and hot gases. Then, if the volume of disk is effectively larger in the late types than in the early types, the late-type spirals may have smaller values of c_* than the early-types because the ISM will travel a larger distance before the mixing. Since $A = a_*/c_*$ and $B = b_*/c_*$, the late type spirals tend to have larger A and B than the early types. Therefore, as an implication, we propose that the size of the disk of galaxies is a factor that physically produces the difference in A and B among the morphologies of spirals.

We expect that the difference in A and B is produced by an interplay between the size effect described in the previous paragraph and the SN rate as mentioned in §4. In fact, the question has been answered from an observational viewpoint in §5.3 of KTC by stating “From an observational point of view, the progression in disk star formation histories with morphological type is not surprising, since one of the fundamental classification criteria is disk resolution, which should relate at least indirectly to the fraction of young stars in the disk.”

In this paper, we present a consistent picture for the variance of star formation activities in spiral galaxies by relating the differences in variance among morphological classes with the supernova rate. However, since an earlier-type sample has a lower gas-to-stellar mass ratio, its

mean SFR will be lower but its variance will in any case tends to be larger because of the stochastic fluctuations. In order to see whether the variance is caused by a purely stochastic process or not, an amplitude of a stochastic SFR should be given in a physically reasonable way. In other words, we should specify what kind of the stochastic process is physically reasonable. Though our model is not stochastic, it provides a way to give an amplitude of the variable SFR. To be fair, however, another modeling for the variation of the SFR, probably a stochastic modeling, may provide another interpretation for the variance of SFR in KTC.

Observational study is now progressing. Recently, Rocha-Pinto et al. (2000) found that the star formation history of the Galaxy is indeed oscillatory. Based on their work, Takeuchi & Hirashita (2000) proposed that the frequency distribution function of the SFR of the Galaxy sampled every 0.4 Gyr from the formation of the Galactic disk shows a flat distribution. Comparing this distribution with the distribution of b in KTC will offer us a useful element in helping to judge whether the scatter of b is caused by an oscillatory behavior of the SFR in any spiral galaxy.

We wish to thank the anonymous referee for invaluable comments that substantially improved the discussion of the paper. We are grateful to S. Mineshige for continuous encouragement. We also thank A. Tomita and T. T. Takeuchi for useful discussions. One of us (HH) acknowledges the Research Fellowship of the Japan Society for the Promotion of Science for Young Scientists. We fully utilized the NASA's Astrophysics Data System Abstract Service (ADS).

REFERENCES

- Cappellaro, E., Turatto, M., Benetti, S., Tsvetkov, D. Yu., Bartunov, O. S., & Makarova, I. N. 1993, *A&A*, 273, 383
- Devereux, N. A., & Hameed, S. 1997, *AJ*, 113, 599
- Habe, A., Ikeuchi, S., & Tanaka, Y. D. 1981, *PASJ*, 33, 23
- Ikeuchi, S., 1988, *Fundam. Cosmic Phys.*, 12, 255
- Ikeuchi, S., Habe, A., & Tanaka, Y. D. 1984, *MNRAS*, 207, 909
- Ikeuchi, S., & Tomita, H. 1983, *PASJ*, 35, 77 (IT83)
- Kamaya, H., & Takeuchi, T. T. 1997, *PASJ*, 49, 471 (KT97)
- Kennicutt, R. C. Jr. 1998, *ApJ*, 498, 541
- Kennicutt, R. C. Jr., Tamblyn, P., & Congdon, C. W. 1994, *ApJ*, 435, 22 (KTC)
- McKee, C. F., & Ostriker, J. P. 1977, *ApJ*, 218, 148
- Nicolis, G., & Prigogine, I. 1977, *Self-Organization in Nonequilibrium Systems* (New York: Wiley and Sons)
- Nozakura, T., & Ikeuchi, S. 1984, *ApJ*, 279, 40

- Nozakura, T., & Ikeuchi, S. 1988, *ApJ*, 333, 68
- Rocha-Pinto, H. J., Scalo, J., Machiel, W., & Flynn, C. 2000, *ApJ*, 531, L115
- Sandage, A. 1986, *A&A*, 161, 89
- Scalo, J. M., & Struck-Marcell, C. 1986, *ApJ*, 301, 77
- Schmidt, M. 1959, *ApJ*, 129, 243
- Tainaka, K., Fukazawa, S., & Mineshige, S. 1993, *PASJ*, 45, 57
- Takeuchi, T. T., & Hirashita, H. 2000, *ApJ*, submitted
- Tomita, A., Tomita, Y., & Saitō, M. 1996, *PASJ*, 48, 285

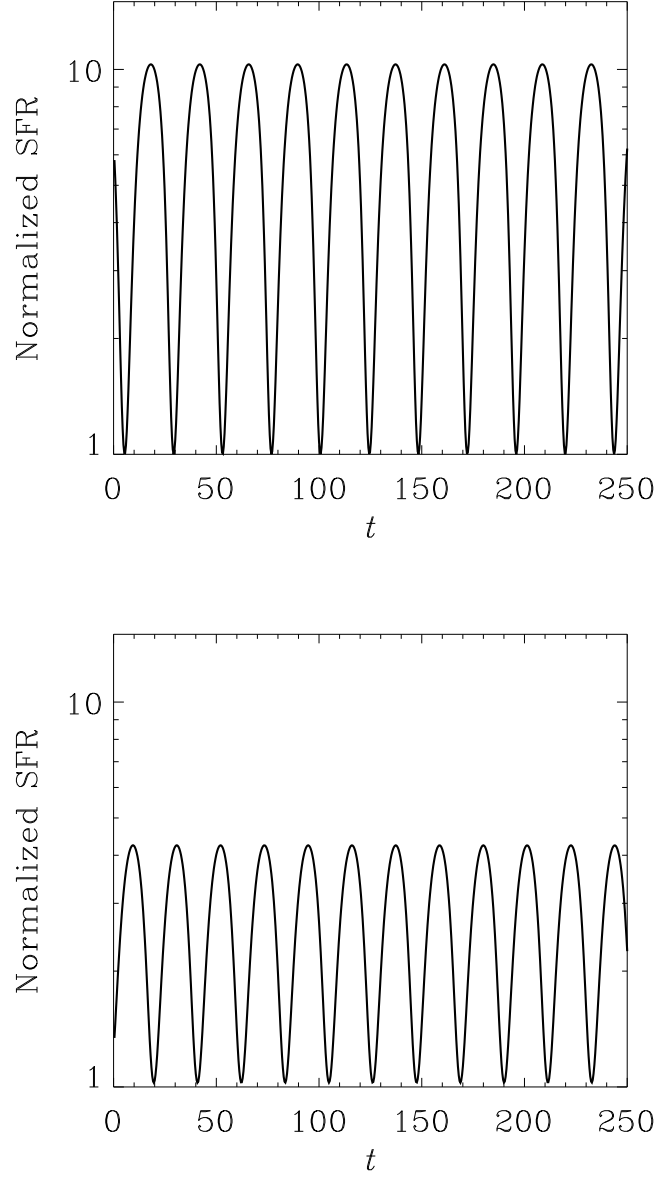


Fig. 1.— Time variation of SFR normalized by the minimum SFR. The timestep is normalized to the cooling time of the hot gas determined by the rate of mixing between hot and warm components ($\sim 10^6$ yr). (a) $A = 0.38$ and $B = 1.0$ are adopted to match the variance of the Sa sample in KTC. The amplitude F_c is 10. (b) $A = 0.40$ and $B = 1.0$ match the variance of the Sc sample in KTC. The amplitude F_c is 4.